

## Infrared diode-laser spectra of the $\nu_9$ and $\nu_{11}$ N–O stretching bands of $\text{N}_2\text{O}_4$

J. L. Domenech, A. M. Andrews, S. P. Belov, G. T. Fraser, and W. J. Lafferty

Citation: *The Journal of Chemical Physics* **100**, 6993 (1994); doi: 10.1063/1.466900

View online: <http://dx.doi.org/10.1063/1.466900>

View Table of Contents: <http://scitation.aip.org/content/aip/journal/jcp/100/10?ver=pdfcov>

Published by the AIP Publishing

### Articles you may be interested in

[Infrared diode laser spectroscopy of the allyl radical. The  \$\nu\_{11}\$  band](#)

*J. Chem. Phys.* **97**, 2963 (1992); 10.1063/1.463037

[Detection of the silylene  \$\nu\_2\$  band by infrared diode laser kinetic spectroscopy](#)

*J. Chem. Phys.* **91**, 4582 (1989); 10.1063/1.456746

[Infrared–microwave double resonance and diode laser spectroscopy of the  \$\nu\_2/\nu\_4\$  bands of  \$\text{SnH}\_4\$](#)

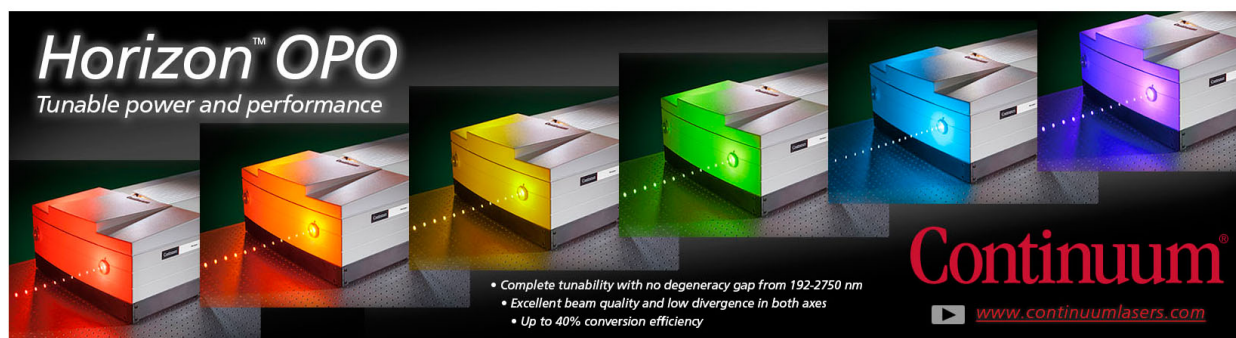
*J. Chem. Phys.* **87**, 5141 (1987); 10.1063/1.453682

[The infrared diode laser spectrum of the  \$\nu\_2\$  band of the  \$\text{FO}\_2\$  radical](#)

*J. Chem. Phys.* **80**, 4694 (1984); 10.1063/1.446534

[Analysis of tunable diode laser spectra of the  \$\nu\_4\$  band of  \$^{12}\text{C}^{13}\text{C}^{16}\text{O}\_2\$](#)

*J. Chem. Phys.* **64**, 2149 (1976); 10.1063/1.432437



**Horizon™ OPO**  
Tunable power and performance

- Complete tunability with no degeneracy gap from 192-2750 nm
- Excellent beam quality and low divergence in both axes
- Up to 40% conversion efficiency

**Continuum®**  
[www.continuumlasers.com](http://www.continuumlasers.com)

# Infrared diode-laser spectra of the $\nu_9$ and $\nu_{11}$ N–O stretching bands of $\text{N}_2\text{O}_4$

J. L. Domenech,<sup>a)</sup> A. M. Andrews, S. P. Belov,<sup>b)</sup> G. T. Fraser, and W. J. Lafferty  
*Molecular Physics Division, National Institute of Standards and Technology, Gaithersburg, Maryland 20899*

(Received 28 October 1993; accepted 4 February 1994)

The rotationally resolved jet-cooled infrared spectra of the  $b$ -type  $\nu_9$  ( $b_{2u}$ ) fundamental band at  $1757\text{ cm}^{-1}$  and the  $a$ -type  $\nu_{11}$  ( $b_{3u}$ ) fundamental band at  $1261\text{ cm}^{-1}$  of the N–O stretches of  $\text{N}_2\text{O}_4$  have been recorded with a diode laser. The  $\nu_9$  band was found to be unperturbed, and it was possible to assign nearly 100% of the observed lines with a signal to noise greater than 2. In contrast, most of the  $K_a$  states of the  $\nu_{11}$  band were found to be strongly perturbed. A large number of strong lines ( $\approx 20\%$ ) are unassigned and presumably arise from the perturbing state as well as torsional hot band transitions. The rotational analysis yields precise spectroscopic constants for the ground vibrational state which are interpreted in terms of a planar centrosymmetric dimer with a N–N bond length of  $1.756(10)\text{ \AA}$ . The observed nuclear-spin statistical weights and near-zero inertial defect are consistent with the planar centrosymmetric structure determined in earlier electron-diffraction studies.

## I. INTRODUCTION

It has been long known that  $\text{N}_2\text{O}_4$  exists in substantial quantities in equilibrium with its monomeric form at room temperature in the gas phase. The enthalpy of formation of  $\text{N}_2\text{O}_4$  in the association–dissociation reaction  $2\text{NO}_2 \rightleftharpoons \text{N}_2\text{O}_4$  ( $\Delta H_0^\circ = -53.2\text{ kJ mol}^{-1}$ ) (Ref. 1) is intermediate between that of a typical covalently bound molecule and a van der Waals complex. The relatively weak binding energy of  $\text{N}_2\text{O}_4$  has made the  $\text{NO}_2/\text{N}_2\text{O}_4$  system attractive for kinetic studies using a variety of techniques such as relaxation methods, flash photolysis, and sound dispersion.<sup>2</sup>

Gas-phase electron-diffraction studies<sup>3</sup> reveal that  $\text{N}_2\text{O}_4$  is a planar centrosymmetric molecule with  $D_{2h}$  point-group symmetry, and a relatively long N–N bond length of  $1.78\text{ \AA}$ , consistent with a weak N–N bond. Matrix-isolation studies<sup>4–9</sup> show evidence for other polar metastable isomers, however, the absence of any deflection of a  $(\text{NO}_2)_2$  beam by an inhomogeneous electric field<sup>10</sup> suggests that these species are not substantially populated in supersonic nozzle expansions.

Because of its center of symmetry,  $\text{N}_2\text{O}_4$  has no permanent electric dipole moment and thus no pure rotational spectrum. The lack of any microwave spectrum for the dimer requires that rotationally resolved vibrational or electronic spectroscopy be used to obtain precise spectroscopic constants for the ground state. The low-resolution infrared spectrum of  $\text{N}_2\text{O}_4$  has been investigated in the gas phase,<sup>11–13</sup> in matrices,<sup>4–9</sup> and in the solid.<sup>14–18</sup> The review by Mélen *et al.*<sup>19</sup> provides a compilation of all the vibrational bands of  $\text{N}_2\text{O}_4$  together with their normal-mode assignments. Perhaps the most detailed investigation in the gas phase is that of Bibart and Ewing,<sup>12</sup> who used vibration-rotation band-shape theory to analyze the infrared absorption features observed

for the dimer. This type of analysis allowed Bibart and Ewing<sup>12</sup> to identify the vibrational symmetries of the observed features, simplifying the normal mode assignments of the absorption peaks. Very recently, Koput, Seibert, and Winniewisser<sup>20</sup> have reported a study of a sequence of weak bands near  $540\text{ cm}^{-1}$  involving a combination of the  $\nu_6$  and torsional energy levels of the type  $[\nu_6 + (n+1)\nu_4] - n\nu_4$ , where  $\nu_4$  is the torsional vibration. They have derived a torsional barrier height of  $1900(200)\text{ cm}^{-1}$ . The work reported in the present investigation was done concurrently with studies by Mélen, Carleer, and Herman,<sup>21</sup> Holland, Carleer, Petrisse, and Herman,<sup>22</sup> and Luckhaus and Quack<sup>23,24</sup> who obtained partially resolved molecular-beam spectra of  $\text{N}_2\text{O}_4$  with Fourier-transform infrared spectrometers.

In the present work we report the high-resolution molecular-beam diode-laser spectrum of the  $\nu_9$  and  $\nu_{11}$  bands of  $\text{N}_2\text{O}_4$ , which are the two strongest of the infrared bands observed by Bibart and Ewing.<sup>12</sup> Bibart and Ewing<sup>12</sup> assigned the  $b$ -type  $\nu_9$  ( $b_{2u}$ ) band to a symmetric combination of the two monomer localized antisymmetric N–O stretches, and the  $a$ -type  $\nu_{11}$  ( $b_{3u}$ ) band to the antisymmetric combination of the two monomer localized symmetric N–O stretches. The present infrared measurements allow the determination of precise ground-state rotational and centrifugal distortion constants for the dimer. The structural results obtained from these constants are in excellent agreement with the earlier electron-diffraction results<sup>3</sup> and recent Fourier-transform infrared molecular-beam measurements<sup>21–24</sup> undertaken simultaneously and independently from the present investigation. Until now, there have been no studies in which the rotational structure of any  $\text{N}_2\text{O}_4$  band has been completely resolved. This is due to the small rotational constants of the molecule, as well as to overlapping lines of hot bands originating in the very low frequency [ $\approx 80\text{ cm}^{-1}$  (Refs. 12,19)] torsional vibration and its overtone levels.

## II. EXPERIMENT

The coupling of diode-laser spectrometers with supersonic molecular-beam sources has been demonstrated to be a

<sup>a)</sup>Visiting Fulbright Fellow. Present address: Instituto de Estructura de la Materia, C.S.I.C., Serrano 119, 28006 Madrid, Spain.

<sup>b)</sup>Permanent address: Molecular Spectroscopy Laboratory, Applied Physics Institute, 46 Ulyanova Street, Nizhny Novgorod, Russia 603024.

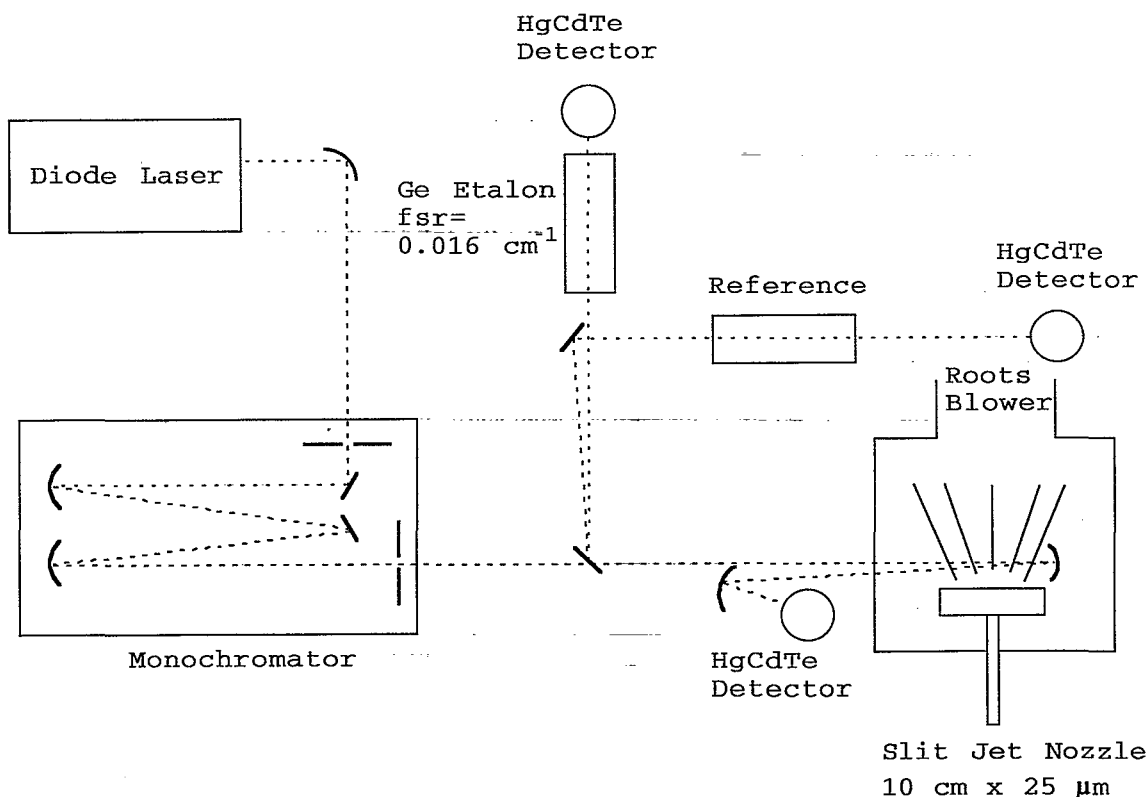


FIG. 1. A schematic diagram of the molecular beam apparatus.

sensitive technique for the spectroscopy of stable molecules and clusters.<sup>25,26</sup> Here, the spectrum of  $\text{N}_2\text{O}_4$  was recorded by measuring the absorption of a diode laser beam by a continuous supersonic expansion of  $\sim 20\%$   $\text{N}_2\text{O}_4/\text{NO}_2$  in Ar through a 10 cm long by  $25\ \mu\text{m}$  wide slit nozzle at a backing pressure of  $\approx 4 \times 10^4$  Pa ( $\approx 300$  Torr). Rotational temperatures are estimated to be around 50 K. The expansion gas was pumped by a roots-blower booster pump backed by a rotary mechanical pump for a total pumping speed of 4000  $\text{m}^3/\text{h}$ .

A schematic diagram of the apparatus is shown in Fig. 1. The experimental configuration evolved substantially between the initial acquisition of the  $1261\ \text{cm}^{-1}$  band and the final acquisition of the  $1757\ \text{cm}^{-1}$  band, so that here only the final “best” instrument setup will be described. Briefly, the rapidly diverging laser radiation from a lead-salt diode is collimated by an off-axis parabolic mirror and sent to a monochromator for single-mode selection and coarse wavelength measurement. Two different laser heads were used, one with a closed cycle He compressor; the other with a liquid-nitrogen cryostat. After the monochromator,  $\sim 10\%$  of the beam intensity is picked off by a  $\text{CaF}_2$  beamsplitter and used to record simultaneous étalon markers and reference-gas calibration spectra. The transmitted light through the étalon and reference gas is monitored using liquid-nitrogen-cooled HgCdTe detectors. The étalon consists of a  $7.6\ \text{cm}$  long ( $\text{FSR}=0.016\ \text{cm}^{-1}$ ,  $\mathcal{F}^*\approx 3$ ) block of germanium.

The main part of the laser beam is directed into the

molecular-beam chamber where it makes two passes through the planar expansion. To minimize the absorption by rotationally warm background gas within the vacuum chamber, the laser beam path outside the jet region is kept to a minimum by placing the input window and the back-reflecting mirror close to the nozzle. After exiting the chamber, the laser beam is focused by an off-axis parabolic mirror onto a HgCdTe detector.

The spectra are taken using the sweep-integration technique first described by Jennings.<sup>27</sup> The diode laser is repetitively swept at  $\sim 800\ \text{Hz}$  over a frequency interval of  $\sim 0.3\ \text{cm}^{-1}$ . Signals from the three detectors are digitized for 500 equally spaced points per sweep at a 1 MHz rate, averaged for 100 sequential sweeps, and stored using a four-channel 350 MHz bandwidth digital oscilloscope, with 8-bit analog-to-digital converters at each input. The molecular-beam absorption channel is simultaneously recorded at 1000 points per sweep using a 10 bit transient recorder, and it is this trace which is used in the final data processing. In this way the narrower line width molecular-beam features are digitized at twice the rate of the other two traces, allowing for a wider scan. All the detectors are ac-coupled to increase the gain for small fractional absorptions of the laser power without amplifying either the signal corresponding to the dc level of the laser power or the background black-body radiation.

The large baseline drift during a scan caused by output-power variations or spatial movement of the laser beam off the detector limits the dynamic range available for capturing

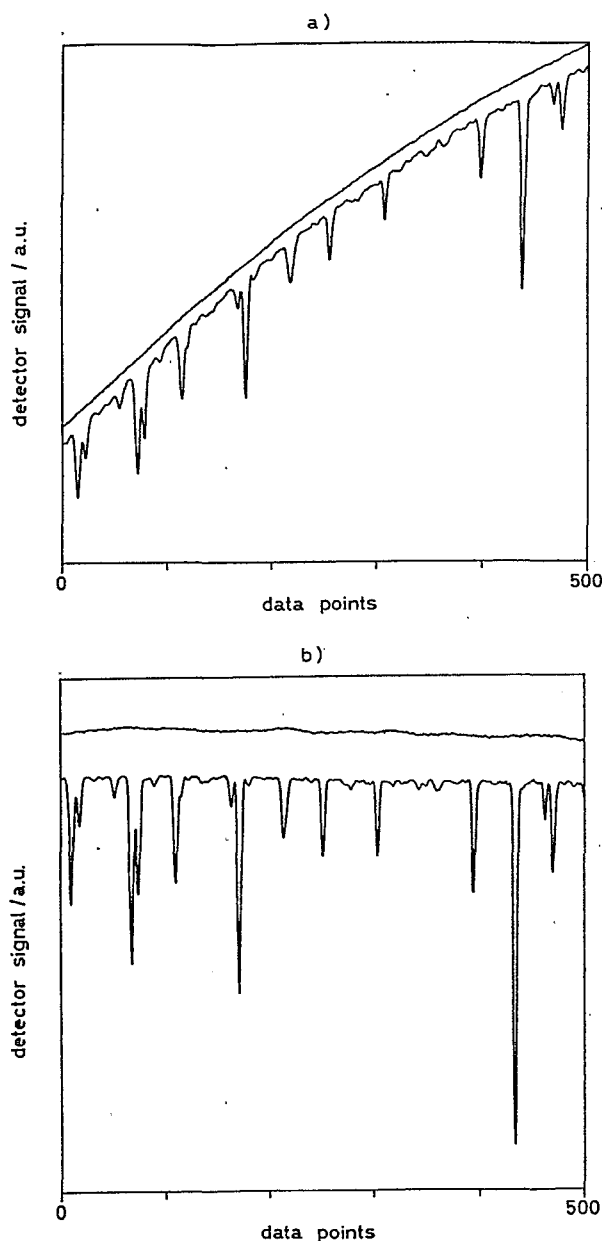


FIG. 2. (a) The upper trace shows the baseline recorded with no sample flowing through the nozzle. The lower trace shows the molecular beam spectrum without baseline correction in an arbitrary region of the  $\nu_{11}$  band of N<sub>2</sub>O<sub>4</sub>. (b) The upper trace shows the result of subtracting the “synthetic” baseline from the upper trace of (a). The lower trace gives the signal recorded when the “synthetic” baseline is subtracted from the molecular beam spectrum. All four traces are the result of averaging 100 consecutive scans.

the absorption signals. As shown in the lower trace of Fig. 2(a), the change of the baseline level during a scan is often larger than many of the absorption lines. If all the lines within a certain spectral window are to be recorded in the same trace, part of the dynamic range of the analog-to-digital converters will be wasted recording the baseline drift, limiting that available for the actual absorption signal. To improve this situation, a real-time baseline subtraction system was built. The signal from the molecular-beam absorption

channel, when there is no gas mixture flowing through the nozzle, is recorded by one of the A/D ports of a 12 bit A/D–D/A board connected to a computer. One hundred consecutive baselines are recorded and averaged in the computer [upper trace of Fig. 2(a)], and this “synthetic” baseline is sent back continuously through a D/A port of the same board, synchronously with the ramp that is driving the laser diode. This signal is filtered to smooth the steps caused by the low throughput of the D/A (100 kHz), and is subtracted in an analog differential amplifier from the true signal coming from the detector, yielding an essentially flat baseline [upper trace of Fig. 2(b)]. The sample spectral absorptions appear superimposed over this flat baseline when the gas mixture is allowed to flow through the nozzle as shown in the lower trace of Fig. 2(b). No effort was made to normalize the absorptions by laser power, which varied with laser frequency, so that observed relative intensities are not quantitative.

In the present experiments two different diodes were used to cover  $\sim 90\%$  of the region between 1256.3 to 1267.0  $\text{cm}^{-1}$  and one diode was used to cover  $\sim 75\%$  of the region between 1749.7–1767.8  $\text{cm}^{-1}$ . Typical noise is  $\sim 10^{-4}$  absorbance units. The full-width at half-height of individual lines were approximately 0.0020 and 0.0011  $\text{cm}^{-1}$  for the  $\nu_9$  and  $\nu_{11}$  bands, respectively.

In the data reduction process, the wave number scale of every spectral trace is linearized by cubic-spline interpolation between the wave number markers provided by the étalon. Traces are recorded so that neighboring spectral windows either from the molecular-beam spectrum or the reference gas spectrum have common absorption lines to key on when merging scans together. Wave number calibration is done by linear interpolation between reference-line positions. The  $\nu_{11}$  band, studied in the range 1256.3–1267.0  $\text{cm}^{-1}$ , falls in the region of the  $\nu_3$  band of N<sub>2</sub>O which provides excellent calibration. Wave numbers, determined by heterodyne measurements, of the lines of this band are given in the calibration tables of Maki and Wells.<sup>28</sup> An estimate of the wave number uncertainty of the lines measured in our work can be obtained from the standard deviation obtained from fitting ground state combination differences. The value of the standard deviation obtained from fitting 155 combination differences obtained from the  $\nu_{11}$  band is 0.000 32  $\text{cm}^{-1}$  with differences as large as 8.4  $\text{cm}^{-1}$  included in the fit. This implies that the measurement uncertainty of a single line is 0.000 23  $\text{cm}^{-1}$ , or about 7 MHz.

In order to obtain suitable calibration for the 1749–1767  $\text{cm}^{-1}$  region, the spectrum of the  $\nu_2$  band of formaldehyde was recorded with a Fourier-transform spectrometer with an apodized resolution of 0.004  $\text{cm}^{-1}$ . This spectrometer was calibrated against lines of H<sub>2</sub><sup>16</sup>O, H<sub>2</sub><sup>17</sup>O, and H<sub>2</sub><sup>18</sup>O recently measured by Toth<sup>29,30</sup> using the Kitt Peak FTS instrument. The formaldehyde band was too sparse to provide complete calibration, and isotopic water lines were used to calibrate frequency ranges not covered by formaldehyde. Ground state combination differences from this band compared favorably with those from the lower frequency band. The combination differences from both bands were combined and fit giving a standard deviation of 0.000 32  $\text{cm}^{-1}$  indicating that the mea-

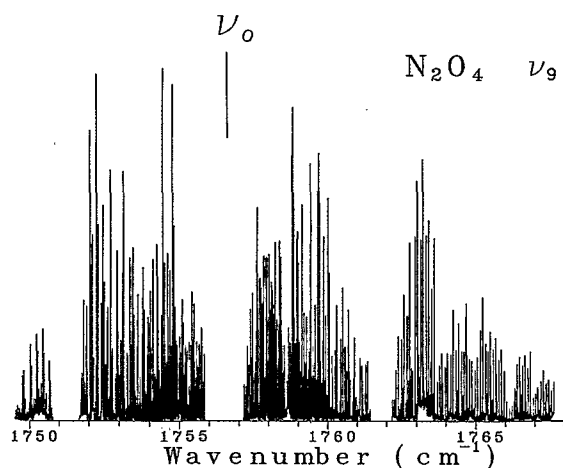


FIG. 3. Spectrum of the  $\nu_9$   $b$ -type band of N<sub>2</sub>O<sub>4</sub>. The gaps in the spectrum centered around 1750.4 and 1760.8 cm<sup>-1</sup> are caused by atmospheric water lines. The gap around the band center at 1756.5 cm<sup>-1</sup> is a region where the diode would not operate.

surement uncertainties from both bands are about equivalent. Measurement of the line wave numbers was greatly facilitated by use of a program written by Carleer.<sup>31</sup>

### III. RESULTS

The  $b$ -type  $\nu_9$  band is centered at 1756.76 cm<sup>-1</sup> in a region of heavy atmospheric water vapor absorption. A compressed plot of the observed spectrum is given in Fig. 3. This figure illustrates the spectral coverage provided by the instrument as well as the band features. The gaps in the spectrum from 1750.8–1751.6 and 1761.4–1762.2 cm<sup>-1</sup> are caused by pressure broadened H<sub>2</sub>O absorption lines while the gap at the band center from 1755.9–1757.2 cm<sup>-1</sup> is a region where the diode does not operate. Lines of the  $\nu_9$  band also fall below 1749.5 cm<sup>-1</sup>, but H<sub>2</sub>O absorption blocks study of the band below this wave number.

The rotational constants calculated from the electron-diffraction structural data reveal that N<sub>2</sub>O<sub>4</sub> is a rather asymmetric top with  $\kappa = (2B - A - C)/(A - C) = -0.37$ . Because of this, the  $Q$ -branches do not form band heads as typically seen in the spectrum of  $b$ -type bands of nearly prolate molecules, and the energy levels of the lower  $K_a$  states approach the oblate limit at low values of the  $J$  quantum number. As a result the  $^rR$ - and  $^pP$  lines form the distinctive patterns that are seen in the wings of perpendicular bands of oblate top molecules. Assignment is also aided (and the spectrum is greatly simplified) by the nuclear-spin statistics which apply to this centrosymmetric molecule. If the molecule is planar, ground state energy levels with  $K_a$  odd are missing. In addition, levels with  $K_c$  even have twice the weight of the levels with  $K_c$  odd. In the oblate rotor patterns observed, all the transitions in one clump of lines have  $K_c$  either all odd or all even producing a strong-weak pattern. This is illustrated in Fig. 4 where a number of these patterns are clearly resolved. A spectrum calculated for a rotational temperature of 50 K is also included in the figure. As discussed below, the observed

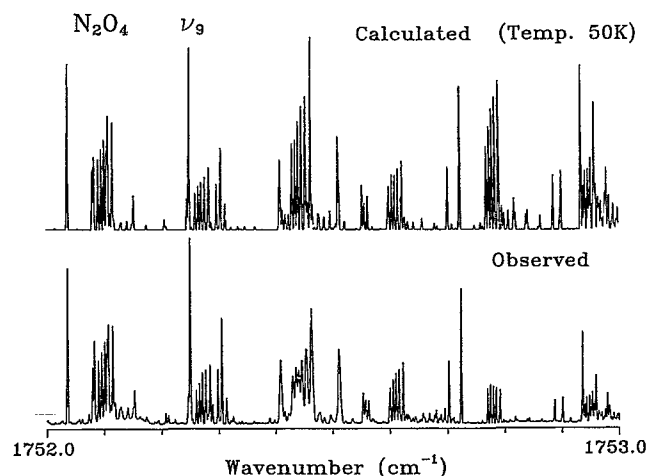


FIG. 4. A 1 cm<sup>-1</sup> portion of the N<sub>2</sub>O<sub>4</sub>  $\nu_9$  band. The panel gives a simulated spectrum calculated at a rotational temperature of 50 K. The bottom panel is the observed spectrum.

line intensities are qualitatively correct but far from quantitative. In addition, the laser line width is not always constant nor always small. For example, the clump of lines at 1752.45 cm<sup>-1</sup> have much greater linewidths than the rest of the lines in the spectrum. (Fortunately this is an extreme case.) The assignment of individual lines in one of the oblate-type clusters is given in Fig. 5. Over 800 lines were assigned in this band; 778 of them were considered unblended and used to determine the spectroscopic constants. Rotational energy levels with  $K_a$  up to 22 and  $J$  up to 50 were observed.

The band origin of  $\nu_{11}$ , an  $a$ -type band with a very strong  $Q$ -branch feature, is at 1262.08 cm<sup>-1</sup>. Figure 6 gives a composite of the complete spectrum. There is no atmospheric interference in this region, and the gaps in the spectrum are areas where the diodes do not function. In the high  $P$ - or  $R$ -branch regions of the band, the spectrum once again resembles a perpendicular band of an oblate top with patterns

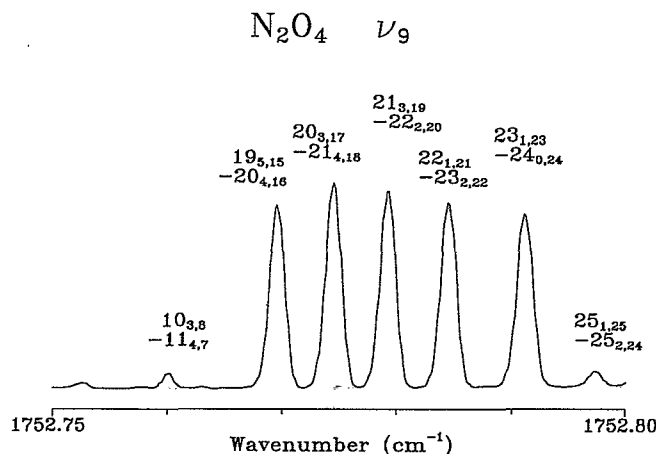


FIG. 5. A 0.05 cm<sup>-1</sup> portion of the spectrum of the  $\nu_9$  band of N<sub>2</sub>O<sub>4</sub> giving the individual line assignments.

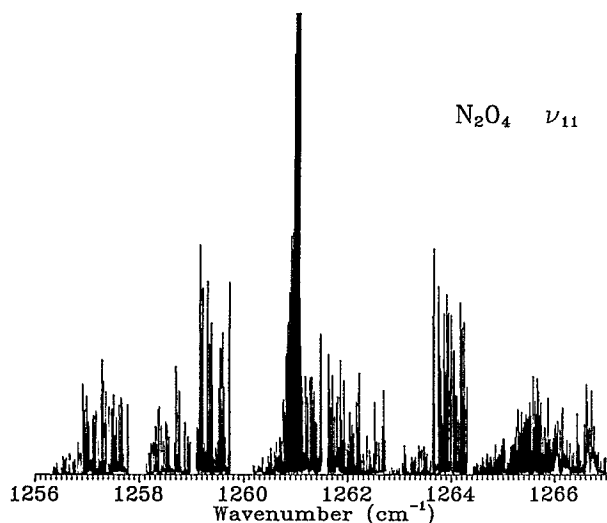


FIG. 6. Spectrum of the  $\nu_{11}$   $\alpha$ -type band of N<sub>2</sub>O<sub>4</sub>. The gaps in the spectrum are where the two available diode lasers do not operate. The irregular line intensities are caused by the method of recording the spectrum (see text).

following the expected strong-weak spin statistics. These patterns are apparent even in the compressed scan given in Fig. 6 in the region 1256.3–1257.8 cm<sup>-1</sup>. Only about 350 unblended lines were assigned in this band since the  $Q$ -branch transitions consisted mainly of unresolved heads. Also the range of observed levels was more restricted with the maximum value of  $J$  being 29 and  $K_a$ , 14. Unlike the higher frequency band, about 20% of the lines were not assigned.

In treating the data, ground state constants were obtained by fitting 690 ground state combination differences, obtained from both bands, with a standard Watson Hamiltonian in the  $I'$   $A$ -representation using a least-squares fitting program writ-

ten by Maki. Combination differences with quantum numbers as high as  $J=42$  and  $K_a=16$  were included in the fit. The standard deviation obtained for the fitting was 0.000 32 cm<sup>-1</sup>. The constants obtained are given in Table I. Besides the on- and off-diagonal quartic centrifugal constants, it was necessary to include all three off-diagonal sextic terms in the fitting. All constants are very well determined.

Once ground state rotational constants were obtained, they were used to calculate upper state term values for both bands, and upper state constants were obtained. The higher frequency  $\nu_9$  band presented no difficulties since only one energy level was found to be perturbed, and transitions involving this level were omitted from the fitting. The upper state spectroscopic constants obtained are also listed in Table I. The standard deviation in fitting 778 lines is 0.000 25 cm<sup>-1</sup>, and the fitting constants obtained are well determined differing only slightly from the ground state constants. The rotational constants obtained are in satisfactory agreement with those derived from the partially resolved spectra reported in Refs. 21 and 24 but are much more precisely determined.

Two transitions in the  $\nu_9$  band with a common upper state,  $37_{3,35}$ – $36_{2,34}$  and  $37_{3,35}$ – $38_{2,36}$ , were perturbation shifted and accompanied by a nearly equally intense “dark” state line. The assignment of these pairs of lines were verified by ground state combination differences. Since the unperturbed line position can be calculated using the derived fitting constants for this band, a value for the magnitude of the matrix element linking the two resonating states can be obtained from the equation,

$$|W| = \frac{1}{2} \sqrt{\Delta E_p^2 - \Delta E_0^2}, \quad (1)$$

where  $W$  is the interaction matrix element,  $\Delta E_p$  is the energy difference of the perturbed energy levels, and  $\Delta E_0$  is the

TABLE I. Spectroscopic constants obtained from the  $\nu_9$  and  $\nu_{11}$  bands of N<sub>2</sub>O<sub>4</sub> in cm<sup>-1</sup>.

	Ground state	$\nu_9$	$\nu_{11}$
$A$	0.217 916 81(177) <sup>b</sup>	0.217 226 705(332) <sup>b</sup>	0.217 532 96(528) <sup>b</sup>
$B$	0.122 332 510(837)	0.121 790 357(235)	0.121 365 09(246)
$C$	0.078 341 902(844)	0.078 111 167 8(153)	0.077 796 05(156)
$\delta_J \times 10^8$	2.350 2(553)	2.327 78(105)	10.580(354)
$\delta_K \times 10^8$	4.839(572)	4.878(135)	41.51(221)
$D_K \times 10^8$	8.032(734)	7.662(113)	12.0(124)
$D_{JK} \times 10^8$	-5.586(501)	-5.955 8(610)	-47.31(381)
$D_J \times 10^8$	6.277 4(830)	6.306 1(161)	29.442(495)
$H_K \times 10^8$			-1.103 6(716)
$H_{KJ} \times 10^8$			1.131 1(436)
$H_{JK} \times 10^9$			-1.088(120)
$h_J \times 10^{13}$	4.70(265)	4.311(251)	58.7(359)
$h_{JK} \times 10^{11}$	1.179(597)	7.796 2(829)	1.179 <sup>c</sup>
$h_K \times 10^{10}$	-2.020(383)	-1.787 8(466)	-2.020 <sup>c</sup>
$\nu_0$		1 756.764 382(23)	1 261.080 227(78)
No. of data	690	778	279
$\sigma$ (cm <sup>-1</sup> )	0.000 32	0.000 25	0.000 40

<sup>a</sup>Perturbed band with effective fitting constants.

<sup>b</sup>Uncertainties are 1 standard deviation.

<sup>c</sup>Constrained to ground state value.

unperturbed separation. The value obtained was 0.004 58(7) cm<sup>-1</sup> which is the average of the values obtained from the *R*- and *P*-branch transitions. This very small matrix element indicates that the resonance must be of very high order. Because of the very low frequency of the torsional vibration in N<sub>2</sub>O<sub>4</sub> the density of states at this frequency is quite large (about 2.7/cm<sup>-1</sup>) making it difficult to identify the source of this accidental crossing.

While the  $\nu_9$  band is virtually unperturbed, the lower frequency  $\nu_{11}$  band is severely perturbed. The  $K_a=0$  and  $K_a=2$  levels with  $K_c$  odd are apparently unperturbed. All the remaining sublevels show a crossing in the range  $J=14-16$ . Unlike the  $\nu_9$  band, many lines remain unassigned in this band. Many of these lines no doubt are perturbation enhanced lines. However the large number of these lines suggests that some originate from hot band transitions associated with the 80 cm<sup>-1</sup> torsional state. No such hot band transitions were seen the  $\nu_9$  region, presumably because they were shifted out of the region of study. All attempts to assign these lines have met with failure. The most likely candidate for the perturbing state is the ternary combination level  $2\nu_6+\nu_{10}$ , which is calculated from the fundamental vibrations to fall within 10 cm<sup>-1</sup> of the fundamental; a  $J_b$ -type Coriolis interaction is possible between  $\nu_{11}$  and this state.

Once the molecular constants were obtained, synthetic spectra were calculated at various temperatures and compared with the observed spectra to determine the rotational temperature in the molecular beam. Due to the uncertainty in the observed intensities, however, this proved to be a rather insensitive method. Estimates of the beam temperature ranged from 20 to 100 K with the most likely value being 50 K.

#### IV. STRUCTURE

Since the N<sub>2</sub>O<sub>4</sub> molecule is nonpolar, it has no microwave spectrum and its structure has not been determined by spectroscopic techniques. The observed spin statistics and the very small positive inertial defect obtained [0.020 43(26)  $\mu\text{\AA}^2$ ] verify the planarity and  $D_{2h}$  symmetry of the molecule. (Observed inertial defects for small planar molecules range from 0.0460  $\mu\text{\AA}^2$  for H<sub>2</sub>O to 0.2629  $\mu\text{\AA}^2$  for Cl<sub>2</sub>CO.<sup>33</sup>) The ground-state rotational constants obtained in this work permit an estimate of the molecular structure for comparison with the structure determined by the electron-diffraction technique. There is insufficient information available from the rotational constants alone to determine a complete  $r_0$  structure, and studying the spectrum of rarer isotopic species would be prohibitively expensive. However, if the assumption is made that the NO<sub>2</sub> group is unchanged in the dimer, a structure of N<sub>2</sub>O<sub>4</sub> can be estimated. In this case a check can be made on this assumption by noting that the ratio  $I_a^{\text{N}_2\text{O}_4}/I_b^{\text{NO}_2}$  equals 1.990 24. If the monomer unit is unchanged in the dimer this ratio should be exactly 2.

Estimates of the center-of-mass distance between the two monomer units,  $r_{\text{cm}}$ , can be obtained using the parallel axis theorem and either  $I_b$  or  $I_c$ ,

TABLE II. Structural parameters of N<sub>2</sub>O<sub>4</sub>.

	This study	Electron-diffraction <sup>a</sup>
$r_{\text{N-N}}$ (Å)	1.756(10) <sup>b</sup>	1.782(8) <sup>c</sup>
$r_{\text{N-O}}$ (Å)	1.196(5)	1.190(2)
$\angle\text{O-N-O}$	133.7(5)°	135.4(6)°

<sup>a</sup>Reference 3.

<sup>b</sup>Estimated uncertainties.

<sup>c</sup>2 $\sigma$ .

$$r_{\text{cm}} = 2 \sqrt{\frac{I_b^{\text{N}_2\text{O}_4} - 2I_a^{\text{NO}_2}}{2M}} = 2 \sqrt{\frac{I_c^{\text{N}_2\text{O}_4} - 2I_c^{\text{NO}_2}}{2M}}, \quad (2)$$

where  $M$  is the molecular weight of NO<sub>2</sub>. The value of  $r_{\text{cm}}$  obtained is 2.410 and 2.405 Å using the  $I_b$  and  $I_c$  inertial constants, respectively. The difference is due to the fact that only ground state inertial constants are available introducing the usual vibrational zero-point errors.

The position of the center of mass of the monomer unit was calculated from the structure of NO<sub>2</sub> using the ground state constants determined by Perrin *et al.*<sup>34</sup> Because of the large inertial defect in NO<sub>2</sub>, the  $r_0$  structure of NO<sub>2</sub> is not well determined, and the average of the parameters obtained from determining the NO<sub>2</sub> structure from the three possible permutations of the inertial constants was used ( $r_0=1.1981$  Å,  $\theta_0=133.96^\circ$ ) to obtain the distance of the N atom from the center of mass of the monomer (0.3259 Å). Taking the average of the values for  $r_{\text{cm}}$  obtained, the value for the N-N bond length obtained is 1.756(10) Å where the uncertainty cited is a realistic estimate of the uncertainties arising from the zero-point effects and the assumptions made. Having fixed this distance, the remaining structural parameters can be estimated using  $I_a$  and  $I_b$ . The structure obtained is given in Table II and compared with the parameters obtained in the electron-diffraction study. The N-N bond length can be compared with the 2.246(1) Å N-N bond length measured in (NO)<sub>2</sub> (Ref. 35) and the 1.864 N-N distance in the N<sub>2</sub>O<sub>3</sub> molecule.<sup>36</sup>

#### V. CONCLUSION

Molecular-beam spectra of the two infrared-allowed N-O stretching vibrations of N<sub>2</sub>O<sub>4</sub>,  $\nu_9$  at 1756.8 cm<sup>-1</sup> and  $\nu_{11}$  at 1261.1 cm<sup>-1</sup>, have been obtained using a diode-laser spectrometer. The rotational structure has been resolved and ground and upper state constants determined. The lower frequency band is highly perturbed; however, the higher frequency stretch is essentially unperturbed and is well characterized with an asymmetric-rotor Hamiltonian. The structure of the molecule has been determined; the N-N bond distance is 1.756(10) Å.

#### ACKNOWLEDGMENTS

A portion of this work was supported by the Upper Atmospheric Research Program of NASA.

<sup>1</sup>A. J. Vosper, J. Chem. Soc. A 1, 625 (1970).

<sup>2</sup>Examples include, T. Carrington and N. Davidson, J. Phys. Chem. 57, 418

- (1953); J. Brunning, M. J. Frost, and I. W. M. Smith, *Int. J. Chem. Kinet.* **20**, 957 (1988); P. Borrell, C. J. Cobos, and K. Luther, *J. Phys. Chem.* **92**, 4377 (1988); B. Markwalder, P. Gozel, and H. van den Bergh, *J. Chem. Phys.* **97**, 5472 (1992).
- <sup>3</sup>B. W. McClelland, G. Gundersen, and K. Hedberg, *J. Chem. Phys.* **56**, 4541 (1972).
- <sup>4</sup>W. G. Fateley, H. A. Bent, and B. Crawford, Jr., *J. Chem. Phys.* **31**, 204 (1959).
- <sup>5</sup>R. V. St. Louis and B. Crawford, Jr., *J. Chem. Phys.* **42**, 857 (1965).
- <sup>6</sup>E. L. Varette and G. C. Pimentel, *J. Chem. Phys.* **55**, 3813 (1971).
- <sup>7</sup>G. R. Smith and W. A. Guillory, *J. Mol. Spectrosc.* **68**, 223 (1977).
- <sup>8</sup>F. Bolduan and H. J. Jodl, *Chem. Phys. Lett.* **85**, 283 (1982).
- <sup>9</sup>H. Bandow, H. Akimoto, S. Akiyama, and T. Tezuka, *Chem. Phys. Lett.* **111**, 496 (1984).
- <sup>10</sup>S. E. Novick, B. J. Howard, and W. Klemperer, *J. Chem. Phys.* **57**, 5619 (1972).
- <sup>11</sup>G. M. Begun and W. H. Fletcher, *J. Mol. Spectrosc.* **4**, 388 (1960).
- <sup>12</sup>C. H. Bibart and G. E. Ewing, *J. Chem. Phys.* **61**, 1284 (1974).
- <sup>13</sup>F. Mélen, F. Pokorni, and M. Herman, *Chem. Phys. Lett.* **194**, 181 (1992).
- <sup>14</sup>B. Andrews and A. Anderson, *J. Chem. Phys.* **14**, 1534 (1981).
- <sup>15</sup>I. C. Hisatsune, J. P. Devlin, and Y. Wada, *J. Chem. Phys.* **33**, 714 (1960).
- <sup>16</sup>F. Bolduan, H. J. Jodl, and A. Loewenschuss, *J. Chem. Phys.* **80**, 1739 (1984).
- <sup>17</sup>A. Givan and A. Loewenschuss, *J. Chem. Phys.* **93**, 7592 (1990).
- <sup>18</sup>A. Givan and A. Loewenschuss, *J. Chem. Phys.* **93**, 866 (1990).
- <sup>19</sup>F. Mélen and M. Herman, *J. Phys. Chem. Ref. Data* **21**, 831 (1992).
- <sup>20</sup>J. Koput, J. W. G. Seibert, and B. P. Winnewisser, *Chem. Phys. Lett.* **204**, 183 (1993).
- <sup>21</sup>F. Mélen, M. Carleer, and M. Herman, *Chem. Phys. Lett.* **199**, 124 (1992).
- <sup>22</sup>J. K. Holland, M. Carleer, R. Petrisse, and M. Herman, *Chem. Phys. Lett.* **194**, 175 (1992).
- <sup>23</sup>D. Luckhaus and M. Quack, *J. Mol. Struct.* **293**, 213 (1993).
- <sup>24</sup>D. Luckhaus and M. Quack, *Chem. Phys. Lett.* **199**, 293 (1992).
- <sup>25</sup>Z. Wang, M. Eliades, and J. W. Bevin, *Chem. Phys. Lett.* **161**, 6 (1989).
- <sup>26</sup>G. D. Hayman, J. Hodge, B. J. Howard, J. S. Muentner, and T. R. Dyke, *J. Chem. Phys.* **87**, 2010 (1987).
- <sup>27</sup>D. E. Jennings, *Appl. Opt.* **19**, 2695 (1980).
- <sup>28</sup>A. G. Maki and J. S. Wells, NIST Spec. Pub. No. 821 (1991).
- <sup>29</sup>R. A. Toth, *J. Opt. Soc. Am. B* **8**, 2236 (1991).
- <sup>30</sup>R. A. Toth, *J. Opt. Soc. Am. B* **9**, 462 (1992).
- <sup>31</sup>M. Carleer, in *Proceedings of the 12th Colloquium of High Resolution Molecular Spectroscopy*, Dijon, France, 1991, edited by J. Moret Bailly (Presses de L'Université de Bourgogne, Dijon 1991), Abstract H21.
- <sup>32</sup>J. K. G. Watson, in *Vibrational Spectra and Structure*, edited by J. R. Durig (Elsevier, Amsterdam, 1977), Vol. 6, pp. 1–80.
- <sup>33</sup>T. Oka and Y. Morino, *J. Mol. Spectrosc.* **11**, 349 (1965).
- <sup>34</sup>A. Perrin, J.-M. Flaud, C. Camy-Peyret, B. Carli, and M. Carlotti, *Mol. Phys.* **63**, 791 (1988).
- <sup>35</sup>C. M. Western, P. R. R. Langridge-Smith, B. J. Howard, and S. E. Novick, *Mol. Phys.* **44**, 145 (1981).
- <sup>36</sup>A. H. Brittain, A. P. Cox, and R. L. Kuczkowski, *Trans. Faraday Soc.* **65**, 1963 (1969).